J|A|C|S
ARTICLES
Published on Web 10/19/2004

Catalytic Mechanism of Yeast Cytosine Deaminase: An ONIOM Computational Study

Stepan Sklenak,[†] Lishan Yao,[†,‡,§] Robert I. Cukier,[†,§] and Honggao Yan*[,†,‡]

Contribution from the Center for Biological Modeling and Departments of Biochemistry and Chemistry, Michigan State University, East Lansing, Michigan 48824

Received June 15, 2004; E-mail: yanh@msu.edu

Abstract: The complete path for the deamination reaction catalyzed by yeast cytosine deaminase (yCD), a zinc metalloenzyme of significant biomedical interest, has been investigated using the ONIOM method. Cytosine deamination proceeds via a sequential mechanism involving the protonation of N^3, the nucleophilic attack of C^4 by the zinc-coordinated hydroxide, and the cleavage of the C^4-N^4 bond. The last step is the rate determining step for the generation of the zinc bound uracil. Uracil is liberated from the Zn atom by an oxygen exchange mechanism that involves the formation of a *gem*-diol intermediate from the Zn bound uracil and a water molecule, the C^4-O^{Zn} cleavage, and the regeneration of the Zn-coordinated water. The rate determining step in the oxygen exchange is the formation of the *gem*-diol intermediate, which is also the rate determining step for the overall yCD-catalyzed deamination reaction.

Introduction

Yeast cytosine deaminase (yCD), a zinc metalloenzyme, catalyzes the hydrolytic deamination of cytosine to uracil (Figure 1). yCD is of great biomedical interest because it also catalyzes the deamination of the prodrug 5-fluorocytosine (5FC), which is one of the most widely used prodrugs for gene-directed enzyme prodrug therapy (GDEPT) for the treatment of cancer.[1] The challenge in cancer therapy is to kill tumor cells without damaging normal cells. GDEPT meets the challenge by activating a prodrug in the tumor, thereby minimizing damage to normal tissues.[1,2] In cytosine deaminase-based GDEPT, the prodrug 5FC is converted to 5-fluorouracil (5FU) by the enzyme. 5FU is an anticancer drug used to treat breast, colon, rectal, stomach, and pancreatic cancers, and is the drug of choice for treating colorectal carcinoma. However, the drug has high gastrointestinal and hematological toxicities. In contrast, the prodrug 5FC is fairly nontoxic to human, because of the lack of the CD activity in human cells. Because humans lack the CD activity, the conversion of 5FC to 5FU only occurs within the tumor. Thus, by producing 5FU in the tumor, the CD/5FC system minimizes toxic effects of 5FU.

The structure of yCD has been recently determined at high resolution with[3,4] and without[4] the inhibitor 2-pyrimidinone, a transition state analogue (Figure 2). yCD is a homodimeric enzyme, and the structure of each monomer consists of a central β-sheet flanked by two α-helices on one side and three α-helices on the other. The homodimeric protein contains two active centers, and each active center is composed of residues within a single subunit and a catalytic zinc ion coordinated with a histidine (His62), two cysteines (Cys91 and Cys94), and a water molecule in the substrate-free enzyme, the latter serving as a nucleophile in the deamination reaction. The inhibitor is bound in a hydrated adduct (4-[R]-hydroxyl-3,4-dihydropyrimidine), and the 4-hydroxyl group is coordinated with the catalytic zinc (Figure 2). The bound inhibitor is completely buried, being covered by a lid composed of Phe114 from the loop between β4 and αD, and Trp152, and Ile156, both from the C-terminal helix. Surprisingly, the structures with and without the transition state analogue are essentially the same with an RMSD of 0.23 Å for the backbone atoms between the two structures. The apo structure contains a second zinc ion at the active site instead. However, the noncatalytic zinc is coordinated with water molecules only and has no direct interactions with the protein. The effects of the noncatalytic zinc on the protein structure are not clear. The yCD-catalyzed reaction is believed to proceed via a tetrahedral intermediate as sketched in Figure 1 with a conserved glutamate (Glu64) serving as a proton shuttle,[3,4] but a detailed mechanism for how the enzyme catalyzes the reaction has not been provided.

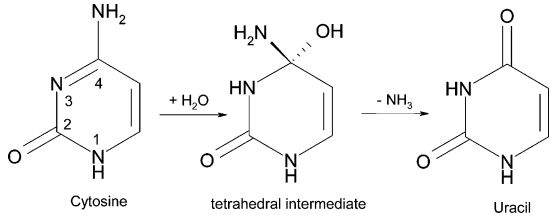

Figure 1. Enzyme cytosine deaminase catalyzes the reaction of cytosine, via the addition of water to form a tetrahedral intermediate, to uracil, with the elimination of ammonia.

The catalytic apparatus of yCD, including the catalytic zinc, its coordinated residues, and the proton shuttle, is very similar to that of *E. coli* cytidine deaminase,[3,4] which has been

[†] Center for Biological Modeling.
[‡] Department of Biochemistry.
[§] Department of Chemistry.

(1) Greco, O.; Dachs, G. U. *J. Cell. Physiol.* **2001**, *187*, 22−36.
(2) Aghi, M.; Hochberg, F.; Breakefield, X. O. *J. Gene Med.* **2000**, *2*, 148−164.
(3) Ko, T. P.; Lin, J. J.; Hu, C. Y.; Hsu, Y. H.; Wang, A. H. J.; Liaw, S. H. *J. Biol. Chem.* **2003**, *278*, 19111−19117.
(4) Ireton, G. C.; Black, M. E.; Stoddard, B. L. *Structure* **2003**, *11*, 961−972.

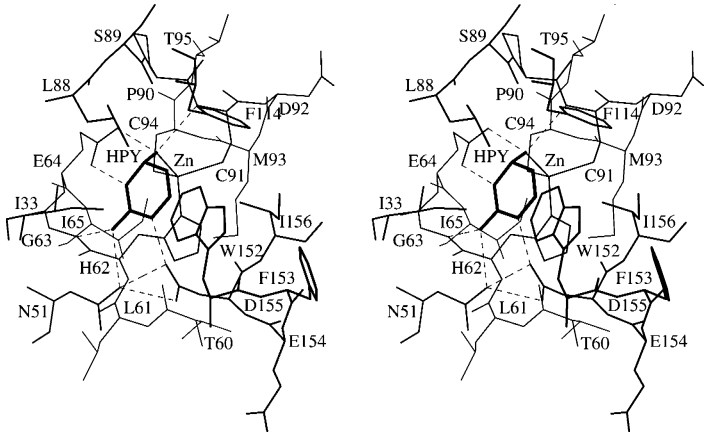

Figure 2. Stereoview of the amino acid residues included in the ONIOM calculations. See Computational methods for the division between the inner and outer layer residues.

extensively studied [5−7] and is a paradigm for understanding enzymatic catalysis. Crystal structures have been determined for the complexes of the enzyme with 3-deazacytidine,[8] 3,4-dihydrozebularine,[9] 3,4-hydrated 2-pyrimidinone riboside,[9] and the product uridine,[10] all at 2.30 Å resolution except the structure of the 3,4-dihydrozebularine complex, which is at 2.20 Å resolution. These crystal structures represent different states of the catalytic cycle and have provided important insights into the catalytic mechanism of the enzyme. However, how the enzyme reaches these states of the catalytic cycle and the energy barriers for the reaction path are not known. Furthermore, none of the analogues can perfectly mimic the substrate and reaction intermediates.

yCD has emerged as another excellent model system for studying this class of enzymatic reactions, because high-resolution structures have been determined (1.14 and 1.60 Å for the two structures of the transition state analogue complex[3,4] and 1.43 Å for the structure without the transition state analogue[4]). Furthermore, yCD is only about half the size of *E. coli* cytidine deaminase and is amenable to high resolution NMR analysis, which is being carried out currently in our laboratory. To understand the catalytic mechanism of yCD, we have performed an ONIOM[11−19] study of the complete reaction path of the enzyme. The enzyme was modeled by 22 amino acid residues divided into two layers. The inner layer was treated by the density functional method B3LYP employing the 6-31G** basis set, and the outer layer by the semiempirical PM3 method. The inclusion of the outer layer was important for obtaining reasonable results for the proposed mechanism. This is a first such study for this class of enzymatic reactions. The results offer significant new insights into the catalytic mechanism of the enzyme.

Computational Methods

A two-layered ONIOM method[11−19] as implemented in the Gaussian program (Gaussian 03)[20] was used in this work. The ONIOM method is a hybrid computational method developed by Morokuma and co-workers that allows different levels of theory to be applied to different parts of a molecular system. In the two-layered ONIOM method, the molecular system under study is divided into an inner and an outer layer. The inner layer consists of the most critical elements of the system, and the rest of the system comprises the outer layer. In the terminology of Morokuma and co-workers, the full system is called "real" and is treated with a low level of theory. The inner layer is termed "model" and is treated with both the low level of theory and a high level of theory. The total ONIOM energy E^{ONIOM} is given by[12,13]

$$E^{\mathrm{ONIOM}} = E(\text{high, model}) + E(\text{low, real}) - E(\text{low, model}) \quad (1)$$

where E(high, model) is the energy of the inner layer (plus the link atoms) at the high level of theory, E(low, real) is the energy of the entire system at the low level of theory, and E(low, model) is the energy of the model system at the low level of theory. Thus, the ONIOM method allows one to perform a high-level calculation on just a small, critical part of the molecular system and incorporate the effects of the surrounding elements at a lower level of theory to yield a consistent energy expression with similar accuracy to a high-level calculation on the full system.

(5) Schramm, V. L.; Bagdassarian, C. K. In *Enzymes, Enzyme Mechanisms, Proteins, and Aspects of NO Chemistry*; Poulter, C. D., Ed.; Amsterdam: New York, 1999; Vol. 5, pp 71−100.
(6) Snider, M. J.; Reinhardt, L.; Wolfenden, R.; Cleland, W. W. *Biochemistry* **2002**, *41*, 415−421.
(7) Snider, M. J.; Lazarevic, D.; Wolfenden, R. *Biochemistry* **2002**, *41*, 3925−3930.
(8) Xiang, S.; Short, S. A.; Wolfenden, R.; Carter, C. W., Jr. *Biochemistry* **1996**, *35*, 1335−1341.
(9) Xiang, S.; Short, S. A.; Wolfenden, R.; Carter, C. W., Jr. *Biochemistry* **1995**, *34*, 4516−4523.
(10) Xiang, S.; Short, S. A.; Wolfenden, R.; Carter, C. W., Jr. *Biochemistry* **1997**, *36*, 4768−4774.
(11) Dapprich, S.; Komaromi, I.; Byun, K. S.; Morokuma, K.; Frisch, M. J. *J. Mol. Struct.* **1999**, *462*, 1−21.
(12) Humbel, S.; Sieber, S.; Morokuma, K. *J. Chem. Phys.* **1996**, *105*, 1959−1967.
(13) Kuno, M.; Hannongbua, S.; Morokuma, K. *Chem. Phys. Lett.* **2003**, *380*, 456−463.
(14) Maseras, F.; Morokuma, K. *J. Comput. Chem.* **1995**, *16*, 1170−1179.
(15) Svensson, M.; Humbel, S.; Froese, R. D. J.; Matsubara, T.; Sieber, S.; Morokuma, K. *J. Phys. Chem.* **1996**, *100*, 19357−19363.
(16) Svensson, M.; Humbel, S.; Morokuma, K. *J. Chem. Phys.* **1996**, *105*, 3654−3661.
(17) Vreven, T.; Morokuma, K. *J. Comput. Chem.* **2000**, *21*, 1419−1432.
(18) Vreven, T.; Mennucci, B.; da Silva, C. O.; Morokuma, K.; Tomasi, J. *J. Chem. Phys.* **2001**, *115*, 62−72.
(19) Vreven, T.; Morokuma, K.; Farkas, O.; Schlegel, H. B.; Frisch, M. J. *J. Comput. Chem.* **2003**, *24*, 760−769.
(20) Frisch, M. J.; Trucks, G. W.; Schlegel, H. B.; Scuseria, G. E.; Robb, M. A.; Cheeseman, J. R.; Montgomery, J. A., Jr.; Vreven, T.; Kudin, K. N.; Burant, J. C.; Millam, J. M.; Iyengar, S. S.; Tomasi, J.; Barone, V.; Mennucci, B.; Cossi, M.; Scalmani, G.; Rega, N.; Petersson, G. A.; Nakatsuji, H.; Hada, M.; Ehara, M.; Toyota, K.; Fukuda, R.; Hasegawa, J.; Ishida, M.; Nakajima, T.; Honda, Y.; Kitao, O.; Nakai, H.; Klene, M.; Li, X.; Knox, J. E.; Hratchian, H. P.; Cross, J. B.; Adamo, C.; Jaramillo, J.; Gomperts, R.; Stratmann, R. E.; Yazyev, O.; Austin, A. J.; Cammi, R.; Pomelli, C.; Ochterski, J. W.; Ayala, P. Y.; Morokuma, K.; Voth, G. A.; Salvador, P.; Dannenberg, J. J.; Zakrzewski, V. G.; Dapprich, S.; Daniels, A. D.; Strain, M. C.; Farkas, O.; Malick, D. K.; Rabuck, A. D.; Raghavachari, K.; Foresman, J. B.; Ortiz, J. V.; Cui, Q.; Baboul, A. G.; Clifford, S.; Cioslowski, J.; Stefanov, B. B.; Liu, G.; Liashenko, A.; Piskorz, P.; Komaromi, I.; Martin, R. L.; Fox, D. J.; Keith, T.; Al-Laham, M. A.; Peng, C. Y.; Nanayakkara, A.; Challacombe, M.; Gill, P. M. W.; Johnson, B.; Chen, W.; Wong, M. W.; Gonzalez, C.; Pople, J. A. *Gaussian 03*, revision B.05; Gaussian, Inc.: Pittsburgh, 2003.

The computational models investigated in this work were based on the 1.14 Å resolution X-ray structure of yCD in complex with the putative transition state analogue 4-[R]-hydroxyl-3,4-dihydropyrimidine (PDB code 1P6O). There are two crystal structures of the complex[3,4] in the Protein Data Bank. We used the 1.14 Å resolution X-ray structure for our calculations because of its higher resolution. The initial structures of the substrate, intermediates and product in the active site were generated from subunit B of the X-ray structure, and the missing atoms were built using the Insight II program (Accelrys, Inc.). The enzyme was modeled as 22 amino acid residues, Ile33, Asn51, Thr60, Leu61, His62, Gly63, Glu64, Ile65, Leu88, Ser89, Pro90, Cys91, Asp92, Met93, Cys94, Thr95, Phe114, Trp152, Phe153, Glu154, Asp155, and Ile156, which form the active site and its surrounding (Figure 2). The calculated systems were divided into two layers. The inner layer, which was treated at the high level of theory, was composed of the substrate or intermediates or product, the imidazole ring (model for His62), Zn, water, ammonia, $CH_3CH_2COO^-$ (model for Glu64) and SCH_3 (model for Cys91 and Cys94). The protonation states of the Zn ligands, cysteine and histidine, are dependent on their surroundings.[21−23] Quantum chemical studies on model compounds show that the Zn−ligand distances are sensitive to their protonation states and, by comparison with crystallographic data, can be reliably assigned.[21,22] Our preliminary calculations revealed that to match the crystal structure, the sulfur atoms of Cys91 and Cys94 must be deprotonated and His62 must be singly protonated. The rest of the system formed the outer layer, which was treated at the low level of theory. Hydrogen atoms were used as link atoms to saturate the dangling bonds.

On the basis of previous ONIOM studies[13,24−28] and our test calculations on the small model of yCD with the bound inhibitor, we chose the density functional method B3LYP[29,30] employing the 6-31G** basis set as the high level. This level of theory and basis set adequately describe the inner part of the enzyme−inhibitor complex with excellent agreement between the calculated and experimental[4] geometries. The semiempirical PM3 method[31,32] was selected as the low level. Karplus and co-workers[33] suggested using quantum chemistry semiempirical methods rather than molecular mechanics schemes to model the protein environment.

The geometry of the inner layer was optimized for all the species, while the atoms of the outer layer were fixed at their crystallographic positions because optimization of the outer layer might lead to an unrealistic expansion of the protein, as found by Morokuma and co-workers.[24] The fact that the structures of yCD with and without the transition state analogue are virtually the same[4] suggests that freezing the outer layer is a reasonable approximation. Furthermore, our preliminary ^{15}N relaxation study also indicates that the backbone of the active center is rigid at picosecond to nanosecond time scales. Because of the size of our system and the fact that the Gaussian program evaluates second derivatives numerically, we used scans to find approximate geometries of the transition states rather than optimization. Consequently, the calculated values of the barriers are their upper bounds.

Results

To elucidate the catalytic mechanism of yCD, two-layer ONIOM (B3LYP:PM3) calculations were performed for a series of yCD-substrate, intermediate, and product complexes. The results are summarized in Figures 3−6 and described in detail below.

Substrate Binding. The reaction pathway of yCD begins with the binding of the substrate, leading to the formation of complexes **1**−**3** (Figure 7a−c). In complex **1** (Figure 7a), Glu64 is deprotonated and the Zn is coordinated with a water molecule. Our DFT calculations on the apo form of yCD indicated that Glu64 cannot deprotonate the Zn-coordinated water molecule without the presence of the substrate. This initial enzyme−substrate complex is stabilized by a network of hydrogen bonds and a π-stacking interaction (Figure 7a). The amino group of cytosine is hydrogen bonded to the carboxyl group of Glu64 and the backbone carbonyl group of Ser89. The carboxyl group of Glu64 is also hydrogen bonded to the Zn-coordinated water, which is in turn hydrogen bonded to the backbone NH group of Cys91. Complex **1** is further stabilized by the interactions of the substrate ring with the rest of the active site residues. These interactions are preserved throughout the course of the deamination reaction. The carbonyl oxygen of the substrate is hydrogen bonded to the side chain amide of Asn51 and the backbone amide of Gly63. The imino group at position 1 of cytosine is hydrogen bonded to the carboxyl group of Asp155. The latter is also hydrogen bonded to the side chain amide of Asn51. The hydrogen bond between the imino group (N^{E2}) of His62 and the backbone carbonyl oxygen of Asp155 helps in maintaining the appropriate orientation of the imidazole ring of His62 that stacks with the cytosine ring.

To form an active enzyme−substrate complex, two proton transfers must occur. First, Glu64 abstracts a proton from the zinc-coordinated water to yield a protonated carboxyl group and a zinc-coordinated hydroxide. In contrast to the apo enzyme, the protonated carboxyl group of Glu64 rotates approximately 120° to form a hydrogen bond with the N^3 atom of cytosine, thus stabilizing the system to give complex **2** (Figure 7b). The zinc bound hydroxide turns ∼140° to form a hydrogen bond with the other oxygen atom of the Glu64 carboxyl group. Complex **2** is calculated to be more stable than **1** by 3.8 kcal/mol at the ONIOM level. The corresponding barrier is negligible (0.6 kcal/mol at ONIOM). On the other hand, **2** is calculated to be *less* stable than **1** by 1.7 kcal/mol based on the *E*(high, model) energy. The difference of 5.5 kcal/mol is the relative stabilization of the model system (the inner layer plus the link atoms) of **2** with respect to **1** by the surrounding protein (the outer layer). There is no barrier found for the rearrangement **1** → **2** on the *E*(high, model) energy surface. The differences between the E^{ONIOM} and *E*(high, model) values manifest the usefulness and importance of the ONIOM scheme, which allows evaluation of the stabilization of the model system by the surrounding protein.

The subsequent proton transfer from Glu64 to N^3 of cytosine yields complex **3** (Figure 7c). The results of our calculations indicate that **3** is more stable than **2** by 3.3 kcal/mol at ONIOM, while it is *less* stable by 7.4 kcal/mol using the *E*(high, model) energy. The difference of 10.7 kcal/mol again indicates the increase of the relative stabilization by protein for the rearrangement **2** → **3**. The corresponding barrier is calculated to be 1.9 kcal/mol at ONIOM. Again, there is no barrier found on the *E*(high, model) energy surface. The very small values of the barriers for the reaction steps **1** → **2** (0.6 kcal/mol) and **2**

(21) Dudev, T.; Lim, C. *J. Phys. Chem. B* **2001**, *105*, 10709−10714.
(22) Dudev, T.; Lim, C. *J. Am. Chem. Soc.* **2002**, *124*, 6759−6766.
(23) Simonson, T.; Calimet, N. *Proteins* **2002**, *49*, 37−48.
(24) Torrent, M.; Vreven, T.; Musaev, D. G.; Morokuma, K.; Farkas, O.; Schlegel, H. B. *J. Am. Chem. Soc.* **2002**, *124*, 192−193.
(25) Cui, Q.; Karplus, M. *J. Am. Chem. Soc.* **2001**, *123*, 2284−2290.
(26) Pawlak, J.; Bahnson, B. J.; Anderson, V. E. *Nukleonika* **2002**, *47*, S33−S36.
(27) Pelmenschikov, V.; Siegbahn, P. E. M. *Inorg. Chem.* **2002**, *41*, 5659−5666.
(28) Lewis, J. P.; Carter, C. W.; Hermans, J.; Pan, W.; Lee, T. S.; Yang, W. T. *J. Am. Chem. Soc.* **1998**, *120*, 5407−5410.
(29) Lee, C. T.; Yang, W. T.; Parr, R. G. *Phys. Rev. B* **1988**, *37*, 785−789.
(30) Becke, A. D. *J. Chem. Phys.* **1993**, *98*, 5648−5652.
(31) Stewart, J. J. P. *J. Comput. Chem.* **1989**, *10*, 209−220.
(32) Stewart, J. J. P. *J. Comput. Chem.* **1989**, *10*, 221−264.
(33) Cui, Q.; Guo, H.; Karplus, M. *J. Chem. Phys.* **2002**, *117*, 5617−5631.

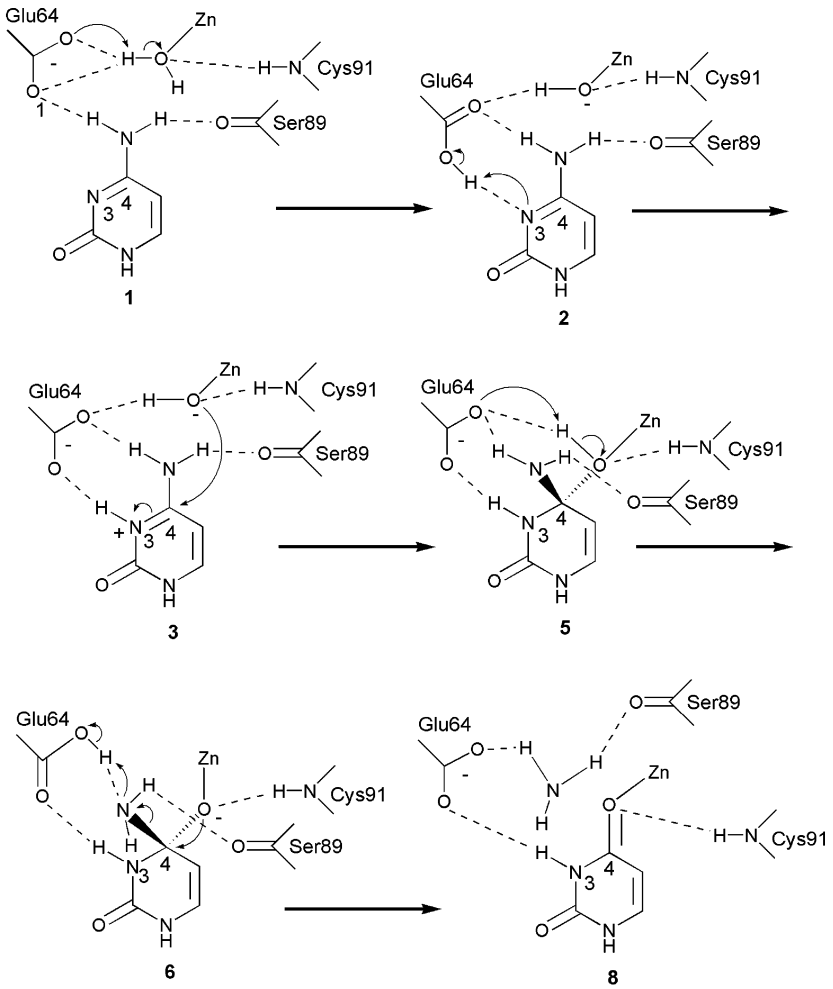

Figure 3. Catalytic pathway for the conversion of cytosine to Zn-coordinated uracil. Only the minima are displayed.

→ **3** (1.9 kcal/mol) indicate that both these glutamate shuttle proton transfers are facile.

Complexes **1**, **2** and **3** differ by the protonation states of Glu64, cytosine, and the zinc-coordinated water. The energy of the complexes progresses in the sequence **1** → **2** → **3** (0.0, −3.8 and −7.1 kcal/mol) at the ONIOM level. On the other hand, the *E*(high, model) energies of **1**, **2** and **3** (0.0, 1.7 and 9.1 kcal/mol) reveal that the stabilization calculated at ONIOM is caused by the increasing stabilization of the model system (the inner layer plus the link atoms) by the surrounding protein (the outer layer) along the sequence **1** → **2** → **3** (0.0, 5.5, and 16.2 kcal/mol). The increasing stabilization of the model system by the surrounding protein reflects the strengthened interactions between amino acid residues at the outer layer and cytosine. It is noted that the orientation of cytosine in complex **1** is somewhat different from that of the transition state analogue in the crystal structure. As complex **1** becomes complexes **2** and **3**, cytosine reorients and superimposes well with the putative transition state analogue in the crystal structure. Therefore, the interactions of the substrate with the amino acid residues at the outer layer strengthen as complex **1** progresses to complexes **2** and **3**.

Hydroxide Nucleophilic Attack. The Zn-coordinated hydroxide in complex **3** is well positioned for the nucleophilic attack on C^4 of cytosine. The distance between the oxygen and carbon atoms decreases from 2.864 Å in complex **1** to 2.437 Å in complex **2** and 2.241 Å in complex **3**. Furthermore, the protonation of cytosine (at N^3) makes the substrate positively charged and so decreases the bond order of the N^3-C^4 bond, which is reflected by the increase of the bond length from 1.336 Å in complex **1** to 1.353 Å in complex **2** and to 1.376 Å in complex **3**. The positive charge in cytosine and the decrease of its N^3-C^4 bond order together with the short distance between O^{Zn} and C^4 make the nucleophilic attack rather facile.

The nucleophilic attack proceeds via transition state **4** to give tetrahedral intermediate **5** (Figure 8a). The approximate geometry of transition state **4** was found by scanning the $O^{Zn}-C^4$ distance with increments of 0.05 Å from complex **3** to tetrahedral intermediate **5**. The maximum was obtained for the $O^{Zn}-C^4$ distance at 1.90 Å. The corresponding reaction barrier is calculated to be 1.0 kcal/mol at ONIOM. Such a low value reveals a very facile reaction. There is no barrier found on the E(high, model) energy surface.

Tetrahedral Intermediates. In complex **5**, the C^4 atom changes its hybridization from sp2 to sp3 during the nucleophilic attack. Tetrahedral intermediate **5** is most closely related to the putative transition state analogue[4] in structure. The only difference is the replacement of the amino group of **5** by a hydrogen atom in the putative transition state analogue. The hydrogen bond network stabilizing the intermediate is unchanged during the nuclephilic attack.

The availability of the crystal structure of the complex of yCD and the putative transition state analogue[4] allows us to

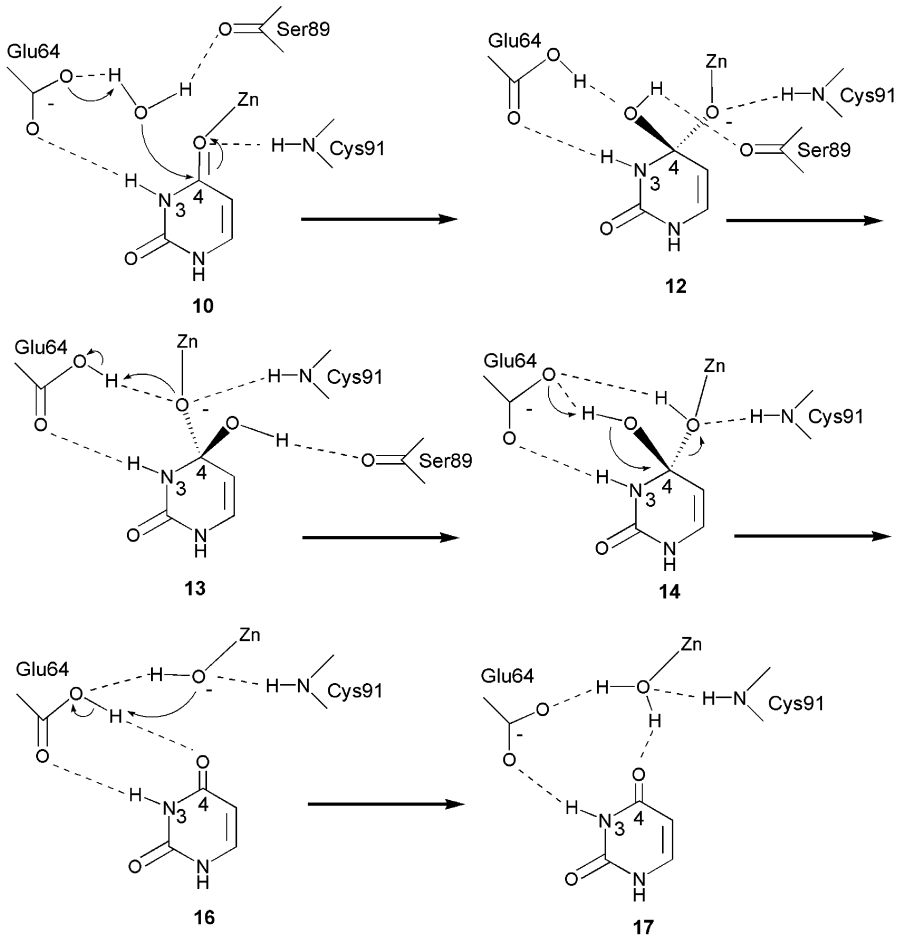

Figure 4. Catalytic pathway for the oxygen exchange to free uracil from the Zn atom. Only the minima are displayed.

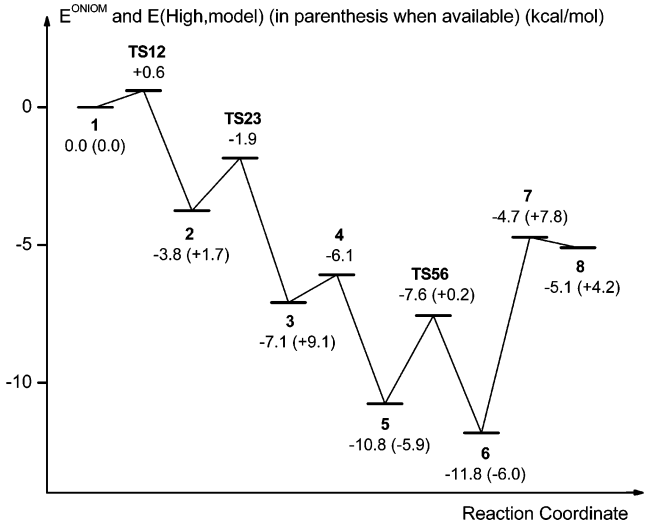

Figure 5. Schematic E^{ONIOM} and E(High,model) energy profile for the conversion of cytosine to Zn-coordinated uracil.

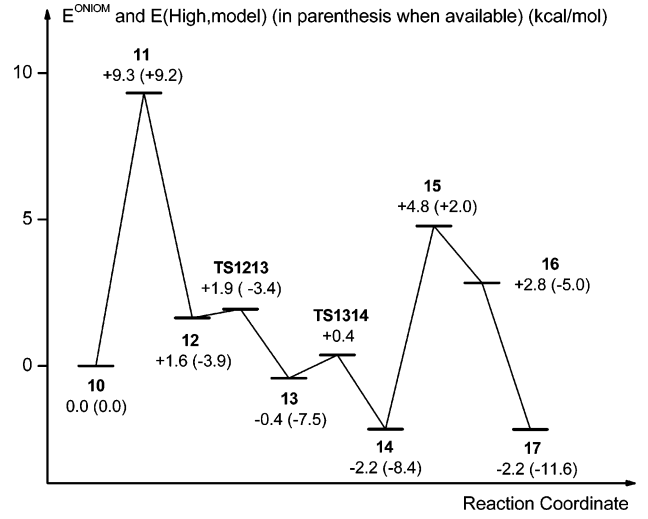

Figure 6. Schematic E^{ONIOM} and E(High,model) energy profile for the oxygen exchange to free uracil from the Zn atom.

compare the calculated and experimentally determined bond lengths, bond and dihedral angles. As summarized in Table 1, the calculated and experimentally determined bond lengths, bond and dihedral angles are in close agreement. The results indicate that the ONIOM(B3LYP:PM3) method is able to adequately determine the structure of **5**, and therefore we can assume that it is able to provide reasonable reaction energies and barriers for the steps of the deamination reaction.

Complex **5** is calculated to be more stable than **3** by 3.7 (ONIOM) and 15.0 kcal/mol (E(high, model)). The difference indicates that the stabilization of **5** relative to **3** calculated at ONIOM (3.7 kcal/mol) is caused by the increasing stability of the model system by 15.0 kcal/mol, whereas the protein environment (the outer layer) reduces that stabilization by 11.3 kcal/mol. In going from **3** → **5**, there is a charge neutralization (**3** has − −+ and **5** has −) that may lead to a loss of

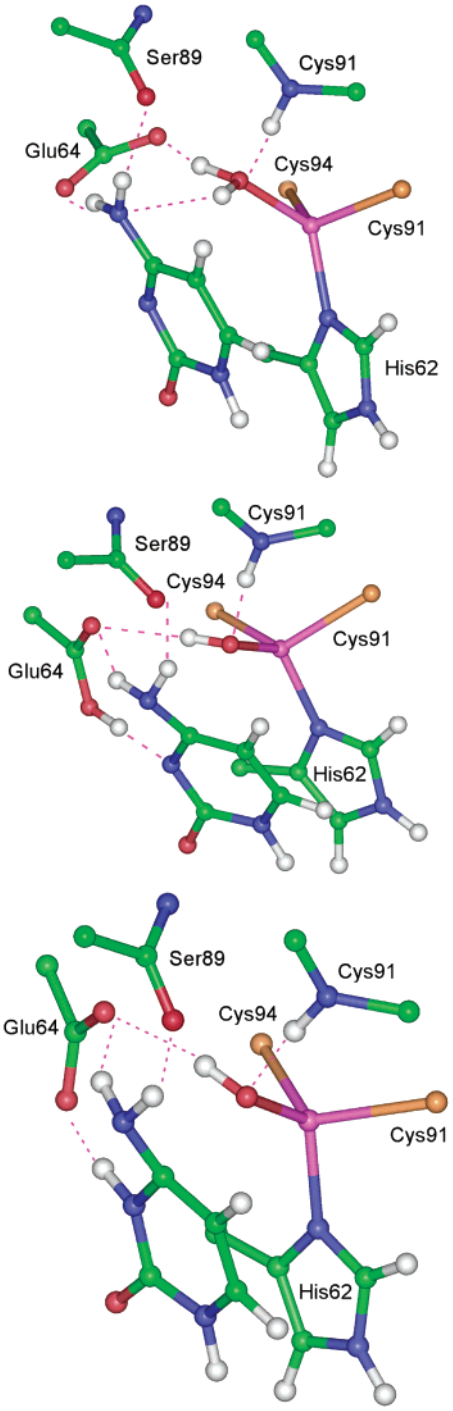

Figure 7. Activation of cytosine by yCD: ONIOM-minimized enzyme substrate complexes **1** (a, top), **2** (b, middle), and **3** (c, bottom). For clarity, only the most critical interactions between the enzyme and substrate are shown.

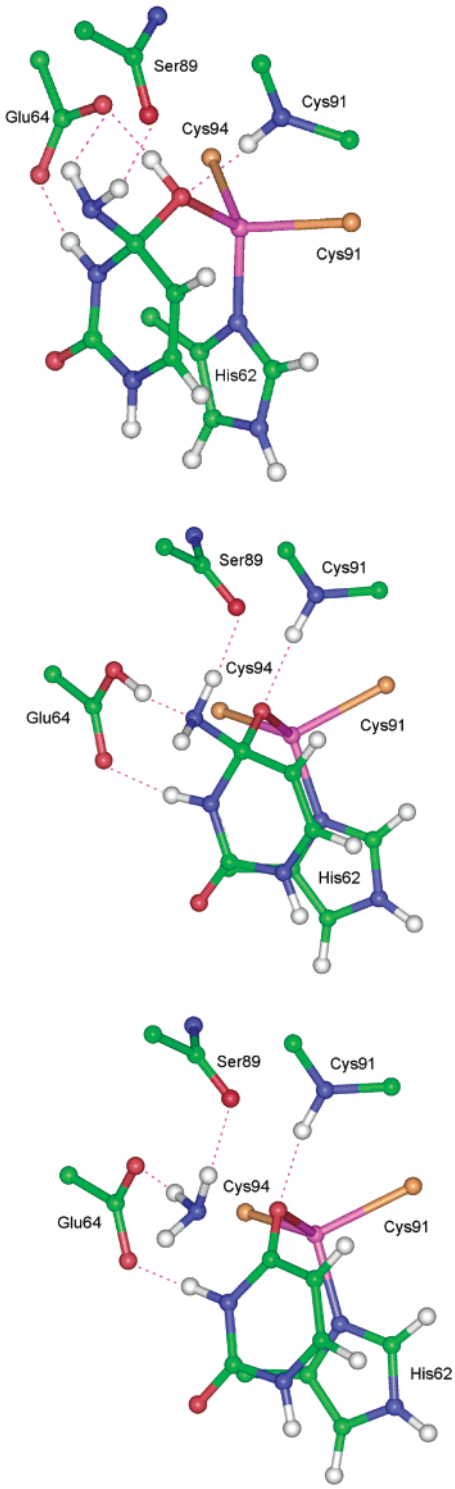

Figure 8. Formation of the tetrahedral intermediates **5** (a, top), **6** (b, middle) and the conversion of **6** to the Zn-coordinated uracil complex **8** (c, bottom).

stabilization energy due to the surroundings in the ONIOM calculation. The charge neutralization mechanism for loss of stabilization energy cannot occur in *E*(high, model) and does not counteract the increased stabilization from formation of the tetrahedral intermediate. This is consistent with the **2** → **3** reaction where now the increased charge separation should lead to stabilization in ONIOM relative to E(high, model), as found.

In order for the reaction to proceed, Glu64 abstracts the proton from the zinc-coordinated hydroxide to form intermediate **6** (Figure 8b). The protonated carboxyl group of Glu64 rotates 26° to form a hydrogen bond with the nitrogen atom of the amino group of the tetrahedral intermediate and thus stabilize the species. **6** is calculated to be more stable than **5** by 1.1 (ONIOM) and 0.1 kcal/mol (*E*(high, model)). The barrier for **5** → **6** is calculated to be 3.2 (ONIOM) and 6.1 kcal/mol (*E*(high, model)).

Formation of the Zinc Bound Uracil and Release of Ammonia. Since the nitrogen atom of the amino group of **6** forms a hydrogen bond with the protonated Glu64, the C^4-N^4

Table 1. Comparison of the ONIOM Optimized Structure of the Tetrahedral Reaction Intermediate (**5**) with the Crystal Structure[4] of the yCD−Inhibitor Complex[a]

internal coordinate	ONIOM	X-ray structure
$Zn-O^{Zn}$	2.055	2.066
$Zn-N^{His62}$	2.006	1.991
$Zn-S^{Cys91}$	2.379	2.302
$Zn-S^{Cys94}$	2.338	2.266
$O^{Zn}-C^4$	1.479	1.475
N^3-C^4	1.446	1.446
$S^{Cys91}-Zn-S^{Cys94}$	115.6°	117.1°
$N^{His62}-Zn-S^{Cys91}$	98.6°	102.0°
$N^{His62}-Zn-S^{Cys94}$	111.9°	113.6°
$N^{His62}-Zn-O^{Zn}$	119.1°	113.1°
$C^2-N^3-C^4-O^{Zn}$	121.2°	114.4°

[a] Bond distances are in Å and angles are in degrees.

bond can be cleaved via transition state **7** to form the zinc bound uracil and ammonia (complex **8**, Figure 8c). A scan of the C^4-N^4 bond with increments of 0.05 Å from **6** to **8** was carried out to locate the approximate geometry of transition state **7**. The maximum was found for the C^4-N^4 distance at 2.10 Å. The corresponding barrier for **6** → **8** is 7.1 kcal/mol at ONIOM. Therefore, the cleavage of the C^4-N^4 bond is calculated to be the rate determining step for the enzymatic deamination reaction from complex **1** to **8**.

On the *E*(high, model) energy surface, the results of the scan calculations reveal that the structure having the C^4-N^4 distance of 1.95 Å is the maximum and the corresponding barrier is 13.9 kcal/mol. This clearly indicates a strong stabilization of the model system of transition state **7** (the inner layer plus the link atoms) by the surrounding protein (the outer layer). The released ammonia forms two hydrogen bonds with the enzyme, one with Glu64 and the other with the backbone carbonyl of Ser89. The C^4-N^4 distance is 2.394 Å. **8** is calculated to be less stable than **6** by 6.7 (ONIOM) and 10.2 kcal/mol (*E*(high, model)). The rate determining reaction step **6** → **8** is calculated to be endothermic. Since ammonia is only loosely bound by two hydrogen bonds to the enzyme, the entropy term for **6** → **8** might make the reaction step more favorable on the free energy surface. In addition, the reaction step **6** → **8** becomes irreversible when ammonia dissociates from the active site.

Release of Uracil from the Active Site. Several ways were envisioned for the release of uracil from the Zn. To find the possible mechanism, two scans of the Zn−O bond were carried out, one in the presence of ammonia and the other without the ammonia, since the ammonia may dissociate first from the active site as in the cytidine deminase catalyzed reaction. The results of the first scan (with ammonia) revealed that increasing the Zn−O distance from the equilibrium value of 2.027 Å (complex **8**) to 3.30 Å produced a monotonic rise of the ONIOM energy from 0 (the relative energy of **8**) to 18.3 kcal/mol.

Before the second scan of the Zn−O bond was performed, the geometry of the uracil−yCD complex (**9**, no ammonia) was optimized. After removing ammonia from the active site, Glu64 abstracts the proton from the N^3 atom of uracil. This deprotonation makes the Zn−O bond cleavage even more difficult. The energy monotonically rises to 19.3 kcal/mol. It is clear from the scan results that there is likely a different mechanism to free uracil.

Alternative Route to Free Uracil from the Active Site. Since there is no available experimental structure of a yCD−uracil complex, we examined the crystal structure of the complex of cytidine deaminase and uridine (PDB code 1AF2; resolution 2.30 Å)[10] for clues for a viable route to free the Zn-coordinated uracil. In the crystal structure, there is a water molecule in the position where ammonia is located in **8**. Since both ammonia and water are small, they may easily move into, as well as out of, the active site. Therefore, it may be possible that after ammonia leaves the active site, a water molecule may move in before the cleavage of the Zn−O bond. To find the structure of the zinc bound uracil−yCD complex with the water molecule, the ammonia molecule in complex **8** was mutated to water and the geometry of the species was optimized. The resultant structure (complex **10**, Figure 9a) is in good agreement with the crystal structure of the complex of cytidine deaminase and uridine[10] when corresponding bond lengths, bond and dihedral angles are compared (Table 2). Uracil is coordinated with the Zn, and the Zn−O distance is 2.061 Å. As with ammonia in complex **8**, the water molecule forms two hydrogen bonds in complex **10**, one with Glu64 and the other with the backbone carbonyl of Ser89.

To find a viable route to free the product, we investigated the possibility of oxygen exchange from the water molecule into uracil. In this scheme, the oxygen atom of the water

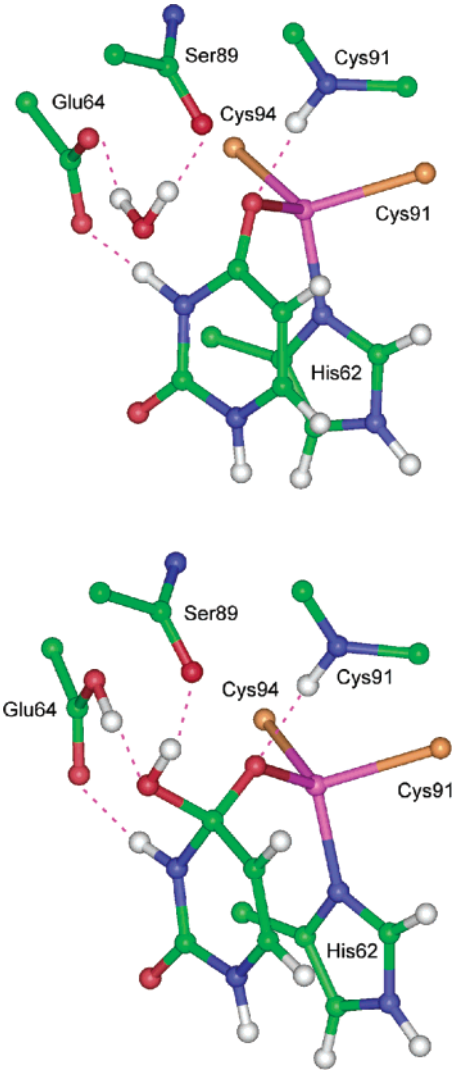

Figure 9. Water bound product complex **10** (a, top) and generation of intermediate **12** (b, bottom).

Table 2. Comparison of the ONIOM Optimized Structure of with the yCD−Uracil Complex (10) with the Crystal Structure[10] of Cytidine Deaminase−Uridine Complex[a]

internal coordinate	ONIOM	X-ray structure
C^4-O^{H2O}	2.590	2.785
$Zn-O^{Zn}$	2.061	2.061
$Zn-N^{His62}$	2.024	2.225
$Zn-S^{Cys91}$	2.371	2.406
$Zn-S^{Cys94}$	2.302	2.120
$O^{Zn}-C^4$	1.266	1.194
N^3-C^4	1.380	1.370
$S^{Cys91}-Zn-S^{Cys94}$	122.0°	109.1°
$N^{His62}-Zn-S^{Cys91}$	100.1°	102.1°
$N^{His62}-Zn-S^{Cys94}$	111.8°	109.7°
$N^{His62}-Zn-O^{Zn}$	112.1°	112.5°
$C^2-N^3-C^4-O^{Zn}$	153.4°	164.1°

[a] Bond distances are in Å and angles are in degrees.

molecule acts as a nucleophile and attacks the C^4 atom of uracil to form a tetrahedral intermediate, whereas Glu64 abstracts a proton from the attacking water in a concerted manner. The tetrahedral intermediate (complex **12**, Figure 9b) subsequently rearranges to generate two more tetrahedral intermediates that are in different protonation states (**13** and **14**, Figure 10). Then the C^4-O^{Zn} bond can be cleaved to free the uracil from the Zn (Complex **16**, Figure 11a) and regenerate the Zn-coordinated water (Complex **17**, Figure 11b).

Oxygen Exchange. The approximate geometry of the transition state for the nucleophilic attack by the water molecule (**11**) was found by scanning the $O^{H2O}-C^4$ distance with increments of 0.05 Å from **10** to tetrahedral intermediate **12**. The maximum was obtained for the $O^{H2O}-C^4$ distance of 1.80 Å (ONIOM) and 1.85 Å (*E*(high, model)). The corresponding barrier for **10** → **12** is 9.3 (ONIOM) and 9.2 kcal/mol (*E*(high, model)). Tetrahedral intermediate **12** (Figure 9b) resembles tetrahedral intermediates **5** and **6** (Figure 8). The two C^4-O bonds have different lengths, 1.349 Å for C^4-O^{Zn} and 1.485 Å for C^4-O^{OH}. The 1.948 Å $Zn-O^{Zn}$ bond in complex **12** is shorter than the same bond in **5** and **10** by some 0.1 Å. The OH group of the tetrahedral intermediate is hydrogen bonded to the protonated carboxyl group of Glu64 and the backbone carbonyl group of Ser89. **12** is calculated to be less stable than **10** by 1.6 kcal/mol at ONIOM and to be more stable by 3.9 kcal/mol on the *E*(high, model) energy surface.

In order for the oxygen exchange to proceed, intermediate **13** (Figure 10a) is formed. The carboxyl group of Glu64 rotates 30° to break its hydrogen bond with O^{OH} and form a new hydrogen bond with O^{Zn}. All other hydrogen bonds are preserved. The calculated barrier for **12** → **13** is very low (0.3 (ONIOM) and 0.4 kcal/mol (*E*(high, model)). The results of our calculations reveal that **13** is more stable than **12** by 2.1 (ONIOM) and 3.7 kcal/mol (*E*(high, model)). The lengths of the two C^4-O bonds in **13** (1.393 Å for C^4-O^{Zn} and 1.432 Å for C^4-O^{OH}) are closer to each other than those in **12**. The 2.005 Å $Zn-O^{Zn}$ bond is longer than the corresponding bond in **12** by some 0.05 Å.

Subsequently, the hydroxyl group of the tetrahedral intermediate rotates 84° to break its hydrogen bond with Ser89 and form a new hydrogen bond with Glu64. Concomitantly, Glu64 protonates the O^{Zn} atom to form intermediate **14** (Figure 10b). The calculated barrier for **13** → **14** is very low (0.8 kcal/mol at ONIOM). There is no barrier found on the *E*(high, model) energy surface. **14** is found to be more stable than **13** by 1.7

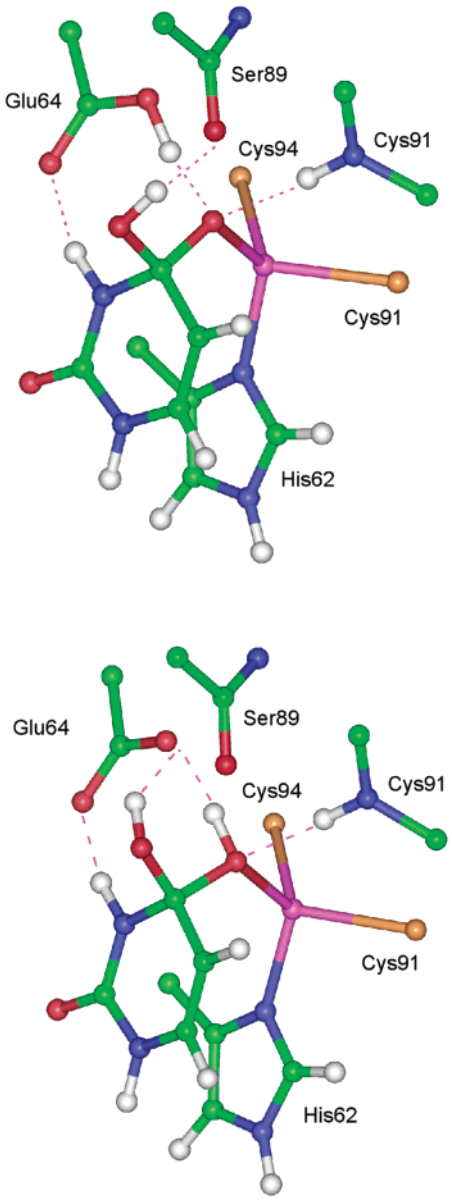

Figure 10. Rearrangement of *gem*-diol intermediate **13** (a, top) by the rotation of the hydroxide group and protonation of O^{Zn} from Glu64 to form **14** (b, bottom).

(ONIOM) and 0.9 kcal/mol (*E*(high, model)). The $O^{Zn}-C^4$ bond of **14** elongates to 1.466 Å, while the $O^{OH}-C^4$ bond shortens to 1.391 Å. The $Zn-O^{Zn}$ bond elongates further to 2.064 Å.

The C^4-O^{Zn} bond is then cleaved to give the free uracil complex (**16**, Figure 11a). The results of our scan of the C^4-O^{Zn} bond from **14** to **16** with increments of 0.05 Å yielded a barrier of 6.9 kcal/mol (ONIOM) and 10.5 kcal/mol (*E*(high, model)). Glu64 abstracts the proton from O^{OH} when the C^4-O^{Zn} distance reaches 2.10 Å, which has the maximum energy for the **14** → **16** scan. **16** is less stable than **14** by 5.0 (ONIOM) and by 3.4 kcal/mol (*E*(high, model)). The $O^{Zn}-C^4$ bond of **16** has been cleaved. The distance between O^{Zn} and C^4 is 2.386 Å and is maintained by the hydrogen bonds between Glu64 and uracil, and between Glu64 and the zinc-coordinated hydroxide (Figure 11a). The uracil molecule in complex **16** is not covalently bound to the enzyme; its orientation in the active site is maintained by interactions with the residues at the outer layer of the system. The $Zn-O^{Zn}$ bond in **16** is 1.898 Å, 0.166 Å shorter than that

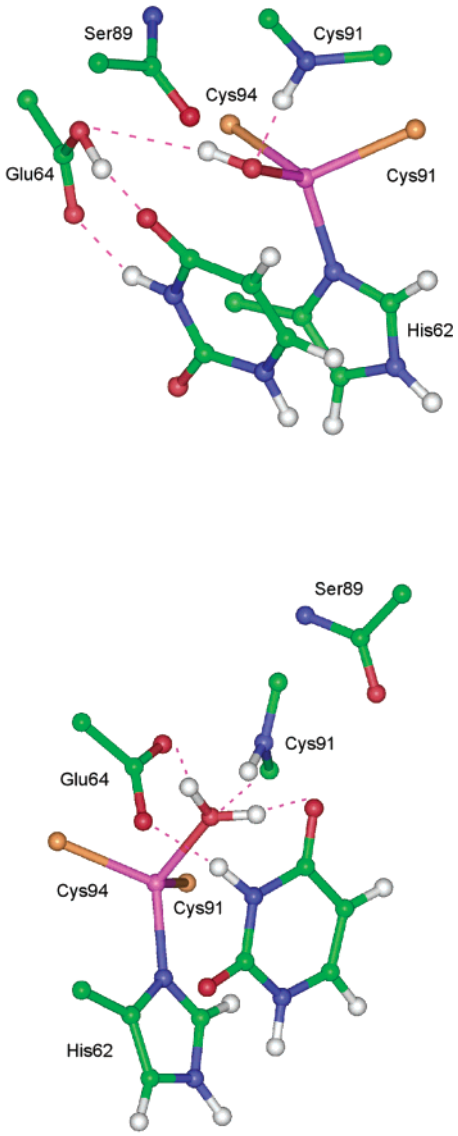

Figure 11. Cleavage of the C^4-O^{Zn} bond of tetrahedral intermediate **14** to yield complexes **16** (a, top) and **17** (b, bottom).

in **14**, because O^{Zn} bears a negative charge. The C^4-O^4 bond length is 1.246 Å, characteristic of a double bond.

Uracil then must move away from the Zn to break the hydrogen bond between O^4 of uracil and Glu64. After breaking the hydrogen bond, the protonated Glu64 is free to rotate and protonate the Zn-coordinated hydroxide to generate complex **17** (Figure 11b). The enzyme is returned to its initial state with a Zn-coordinated water. The $O^{Zn}-C^4$ distance in **17** increases to 2.770 Å, and the C^4-O^4 bond length is slightly shortened to 1.231 Å. Since O^{Zn} no longer bears a negative charge, the $Zn-O^{Zn}$ bond is elongated to 1.990 Å. The results of our calculations reveal that **17** is more stable than **16** by 5.0 (ONIOM) and 6.6 kcal/mol (*E*(high, model)).

The barriers summarized in Figures 5 and 6 show that the nucleophilic attack of water on the zinc bound uracil (**10** → **12**) is calculated to be the rate determining step for the oxygen exchange, as well as for the entire catalyzed deamination reaction going from cytosine−enzyme complex **1** to the free product **17**.

Discussion

The results of the ONIOM study presented here provide an atomistic and energetic description of the reaction path for yCD (Figures 3−6). Although little is known about its catalytic mechanism and few mechanistic studies have been reported on the enzyme, there have been many studies of *E. coli* cytidine deaminase.[5−7] As described earlier, the catalytic apparatus of yCD is very similar to that of the cytidine deaminase.[3,4] Therefore, the two enzymes are likely to have very similar catalytic mechanisms. This allows us to corroborate our findings by comparison with those on the cytidine deaminase reaction, and shed new light on this class of enzymatic reactions.

Reaction Path and Rate Determining Steps. The reaction path of yCD can be divided into three stages: the formation of tetrahedral intermediate **5** (Figure 8a), the cleavage of the C^4-N^4 bond to generate a Zn-coordinated uracil (complex **8**, Figure 8c), and the cleavage of the C^4-O^{Zn} bond to free the uracil from the Zn (complex **17**, Figure 11b). The formation of the tetrahedral intermediate follows a stepwise mechanism. Glu64 extracts a proton from the Zn-coordinated water first and then protonates the N^3 atom of cytosine. The resultant Zn-coordinated hydroxide then attacks the C^4 atom of cytosine to yield the tetrahedral intermediate **5**. The process is a facile one with small energy barriers (Figure 5). As an alternative pathway, a concerted mechanism in which protonation of N^3 is concomitant with the attack of C^4 by the Zn-coordinated hydroxide was also investigated. The result of this study indicates that the formation of the tetrahedral intermediate follows a stepwise mechanism, because the concerted mechanism has much a higher energy barrier (5.3 kcal/mol, data not shown). The stepwise mechanism is consistent with a large scale semiemprical quantum mechanical (PM3) study of the substrate complex of *E. coli* cytidine deaminase.[28,34] The so-called active species of the substrate complex of the cytidine deaminase is protonated at the N^3 of cytidine and the Zn-coordinated water is deprotonated, a result that is very similar to complex **3** in our study. Protonation of N^3 greatly facilitates the nucleophilic attack by the Zn-coordinated hydroxide on C.[4]

The conversion of the tetrahedral intermediate (**5**) to the Zn bound uracil (complex **8**, Figure 8c) is also a stepwise process with Glu64 first deprotonating HO^{Zn} (complex **6**). However, protonation of the amino group of the tetrahedral intermediate and the cleavage of the C^4-N^4 bond are concerted. This is the rate determining step in the conversion of cytosine to the Zn bound uracil. The energy barrier is 7.1 kcal/mol at ONIOM, much higher than that for the formation of the tetrahedral intermediate (**5**). The result is consistent with the significant ^{15}N kinetic isotope effects on the cleavage of the C^4-N^4 bond of cytidine.[6]

In order for uracil to dissociate from the active site of the enzyme, the $Zn-O^{Zn}$ bond must be cleaved first. It is surprising that the cleavage of the $Zn-O^{Zn}$ is so difficult, with an energy barrier at least 18 kcal/mol in the presence of ammonia and 19 kcal/mol in the absence of ammonia. We found that oxygen exchange is a viable route to free the Zn bound uracil, instead of cleavage of the $Zn-O^{Zn}$ bond. In this mechanism, with the assistance of Glu64, a water molecule attacks the C^4 atom to form a *gem*-diol tetrahedral intermediate and the subsequent cleavage of the C^4-O^{Zn} bond frees uracil from the Zn and regenerates the Zn-coordinated water. The highest energy barrier in the process is 9.3 kcal/mol (ONIOM) for the formation of

(34) Lewis, J. P.; Liu, S. B.; Lee, T. S.; Yang, W. T. *J. Comput. Phys.* **1999**, *151*, 242−263.

tetrahedral intermediate **12**, 2.2 kcal/mol higher than the energy barrier for the cleavage of the C^4-N^4 bond. The formation of the *gem*-diol tetrahedral intermediate is the rate-determining step not only in the oxygen exchange but also in the entire course of the yCD-catalyzed deamination reaction. That oxygen exchange route is a viable mechanism for freeing uracil from the Zn atom is based on several lines of reasoning: (1) although the energy barrier for the oxygen exchange is high, it is much lower than that for the direct cleavage of the $Zn-O^{Zn}$ bond as described earlier; (2) the closely related enzyme cytidine deaminase catalyzes the exchange of water into uracil, and adenosine deaminase also catalyzes the exchange of water into inosine;[35] (3) the aforementioned ^{15}N kinetic isotope effects are not fully manifested in the wild-type cytidine deaminase-catalyzed deamination reaction, indicating that there is another step influencing the rate besides the slow C^4-N^4 bond cleavage;[6] and (4) transient kinetic analysis has shown that product release is rate-determining in the yCD-catalyzed reaction (Y. Li et al., personal communication).

Role of Glu64. Glu64 is the key residue in yCD catalysis. Indeed, when the corresponding glutamate residue in *E. coli* cytidine deaminase was mutated to alanine, the k_{cat} of the enzyme was reduced by 8 orders of magnitude.[36] However, the mutagenesis study did not reveal the exact role of the residue. Our ONIOM calculations reveal that Glu64 serves as a proton shuttle four times during the course of the deamination reaction. First, Glu64 abstracts one proton from the zinc bound water in complex **1** and transfers it to N^3 of cytosine in complex **3**. Second, Glu64 abstracts the proton of the zinc bound hydroxide (complex **5**) and donates it to the amino group of cytosine concomitantly with the cleavage of the C^4-N^4 bond to yield ammonia and the Zn bound uracil (complex **8**). Third, during the oxygen exchange to free uracil from the Zn atom, Glu64 deprotonates the water molecule for nuleophilic attack at the C^4 atom of the zinc bound uracil (complex **10**) in a concerted manner to generate a tetrahedral intermediate (complex **12**) and delivers it to O^{Zn} (complex **14**). Finally, when the C^4-O^{Zn} bond is cleaved to free uracil from the Zn (complex **16**), Glu64 abstracts the proton from the hydroxyl group of the tetrahedral intermediate in a concerted manner and delivers it to the Zn-coordinated hydroxide and regenerates a Zn-coordinated water (complex **17**).

Stabilization of the Reaction Species by the Enzyme. It is well-known that active site residues besides those directly involved in chemistry play important roles in enzymatic catalysis.[37] The ONIOM methodology we employed in our calculations is particularly useful for capturing the contributions of these residues to catalysis.[11−19] It allowed us to model large parts of the enzyme rather than just a few functional groups that are directly involved in chemistry as in pure ab initio or DFT calculations. The ONIOM scheme provides two different energetic terms − the ONIOM and *E*(high,model) energies (see eq 1). The ONIOM energy, which includes the interaction of the reaction species with the enzyme, is the energy that should be used to describe the barriers and energies for the reaction path of the enzymatic reaction. The *E*(high, model) energy only serves to illustrate the effect of the enzyme on the reaction species, since the difference between the ONIOM and *E*(high, model) energies is the stabilization or destabilization of a particular reaction species by the surrounding residues. The barrier for the reaction step **6** → **8** is calculated to be significantly lower at ONIOM than on the *E*(high, model) energy surface. The corresponding values are 7.1 and 13.9 kcal/mol, respectively. The difference of 6.8 kcal/mol illustrates a stronger stabilization of transition state **7** than intermediate **6**. Similarly, the calculated barrier for **14** → **16** is lower by 3.6 kcal/mol at ONIOM. On the other hand, the barrier for **10** → **12** has essentially the same value at both levels since the stabilization of **10** and transition state **11** is the same. Several times there was no barrier found for a reaction step on the *E*(high, model) energy surface. The results highlight the importance of including the interaction of the model system with the surrounding protein. The stabilization of the reaction species by the surroundings reflects the strengthened interactions of the reaction species with the surrounding residues. For example, with an N−O distance of 3.14 Å and an N−H−O angle of 156°, the hydrogen bond between the amino group of the tetrahedral intermediate with the carbonyl group of Ser89 in complex **6** is rather weak. When in transition state **7**, the N−O distance shortens to 2.91 Å, the N−H−O angle becomes 168°, and therefore the hydrogen bond becomes much stronger. Similarly, the hydrogen bond between O^{Zn} and the backbone amide of Cys91 is 3.01 Å in complex **14** and shortens to 2.82 Å in transition state **15** and becomes stronger in the transition state.

Conclusions

The complete path of the yCD-catalyzed deamination reaction has been described by a two-layered ONIOM(B3LYP:PM3) study. The substrate is first activated by protonation at the N^3 position. The proton is transferred from the Zn-coordinated water to cytosine via Glu64. The zinc-coordinated hydroxide then attacks C^4 of the protonated cytosine to yield a tetrahedral intermediate. Subsequently, the C^4-N^4 bond is cleaved to form ammonia and zinc bound uracil. The formation of the tetrahedral intermediate is facile, and the C^4-N^4 bond cleavage is the rate determining step (with barrier 7.1 kcal/mol at ONIOM) for the generation of the zinc bound uracil. Because the energy barrier for the $Zn-O^{Zn}$ cleavage is very high (≫18 kcal/mol), an alternative mechanism involving oxygen exchange was investigated and shown to provide a viable route for liberating uracil from the Zn. The oxygen exchange mechanism features the formation of a *gem*-diol intermediate from the Zn bound uracil and a water molecule, the C^4-O^{Zn} cleavage, and the regeneration of the Zn-coordinated water. The rate determining step in the oxygen exchange is the formation of the *gem*-diol intermediate with a barrier of 9.3 kcal/mol at ONIOM, which is also the rate determining step for the overall yCD-catalyzed deamination reaction. General acid/base catalysis plays an important role throughout the course of the deamination reaction, and Glu64 is responsible for all the proton transfers. The results also showed the importance of including the interactions of the reaction species with the surrounding protein in computational studies of enzymatic catalysis.

Acknowledgment. The work is supported in part by the Center for Biological Modeling of Michigan State University

(35) Shih, P.; Wolfenden, R. *Biochemistry* **1996**, *35*, 4697−4703.
(36) Carlow, D. C.; Smith, A. A.; Yang, C. C.; Short, S. A.; Wolfenden, R. *Biochemistry* **1995**, *34*, 4220−4224.
(37) Fersht, A. R. *Structure and Mechanism in Protein Science*; Freeman: New York, 1999.

and NIH grants (GM58221 to H.Y. and GM47274 to R.I.C.).

Supporting Information Available: The calculated absolute ONIOM and *E*(high, model) energies of all the species and figures of species **4**, **7**, **9**, **11**, and **15** are available. This material is available free of charge via the Internet at http://pubs.acs.org.

JA046462K